EAM Integrated Widely Tunable DBR Lasers Based on InGaAlAs/InP MQWs

Mengyang Zhong, Huan Li, Daibing Zhou, Kun Yang, Fei Guo, Dan Lu, Lingjuan Zhao, and Song Liang

***Abstract*—We report the fabrication of a first electro-absorption modulated widely tunable DBR lasers (TEML) based on InGaAlAs multi-quantum well (MQW) material, which is superior than InGaAsP MQWs for the fabrication of both modulators and lasers. The device is fabricated by using butt-joint material growth technology and operates at a wavelength of 1.5 μm. An over 12 nm wavelength tuning range can be obtained. The characteristic temperature of the device is 83 K, which is notably higher than that for a laser based on InGaAsP MQWs. At 25°, the electro-absorption modulator (EAM) of the device has a small signal modulation bandwidth exceeding 27 GHz, which is notably higher than the bandwidth for a TEML device having the same structure but InGaAsP MQW active material. At 25 Gb/s NRZ data modulation, to achieve 10E-10 bit error rate (BER), the power penalty after 5 and 10 km fiber transmission are 1 and 3 dB, respectively. The device is a promising low-cost light source for future high-capacity wavelength division multiplexing (WDM) optical communication systems.**

***Index Terms*—Electro-absorption modulator, distributed Bragg reflector (DBR) laser, multiple quantum wells.**

I. Introduction

With the rapid development of the Internet, there is an escalating demand for increasing the capacity of optical networks [1], [2], [3], [4]. High quality light sources are key components for optical communication systems. Semiconductor lasers are widely used light sources, because of their advantages including low power consumption, compact size, and high reliability. Distributed feedback lasers, either directly modulated or electro-absorption modulated can be adopted [5], [6], [7]. However, their wavelength tuning range is limited. For wavelength division multiplexing (WDM) systems, which increase the data capacity by transmitting multiple different wavelengths at the same time, a number of these devices each having a different wavelength have to be used, which would inevitably increase the system's construction costs. Distributed Bragg Reflector (DBR) lasers have been gaining increasing attention due to their simple tuning method and easy fabrication process, as compared to the external cavity lasers [8] and sampled grating DBR lasers [9]. High-speed modulated DBR lasers are promising low cost devices to meet the demands for high capacity WDM optical communication systems [10], [11].

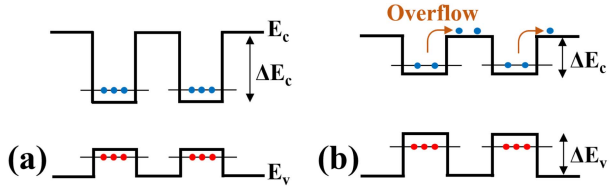

Fig. 1. Quantum well band diagrams of InGaAlAs (a) and InGaAsP (b) [12].

Electro-absorption modulated tunable DBR lasers (TEML) have been demonstrated in previous works [11], [13], [14]. High speed data can be transmitted for a longer distance by using these externally modulated lasers than using directly modulated DBR lasers [10]. However, all the reported TEML devices are based on InGaAsP/InP multi quantum well material up to now. In this paper, we report for the first time to the best our knowledge, the fabrication of TEML devices based on InGaAlAs MQW material, which is superior than InGaAsP MQWs for the fabrication of both the modulator and laser [15], [16], [17]. As shown in Fig. 1, compared to InGaAsP MQWs, InGaAlAs MQWs have larger conduction band offset between wells and barriers which leads to a better electron confinement in the wells [18]. For the fabrication of lasers, this leads to a better high temperature performance. For EAM, the application of InGaAlAs MQWs enhances the quantum confined Stark effect, thus leading to a better modulator performance [19]. The device is fabricated

Manuscript received 11 February 2024; revised 3 May 2024; accepted 23 May 2024. Date of publication 28 May 2024; date of current version 15 October 2024. This work was supported in part by the National Key Research and Development Program of China under Grant 2021YFB2206501, in part by the Strategic Priority Research Program of Chinese Academy of Sciences under Grant XDB43000000, and in part by the National Natural Science Foundation of China under Grant 62274156. *(Corresponding authors: Daibing Zhou; Song Liang.)*

Mengyang Zhong is with the College of Electronic Information, Zhengzhou University of Light Industry, Zhengzhou 450000, China, also with the Key Laboratory of Optoelectronic Materials and Devices, Institute of Semiconductors, Chinese Academy of Sciences, Beijing 100083, China, also with the Center of Materials Science and Optoelectronics Engineering, University of Chinese Academy of Sciences, Beijing 100049, China, and also with the Beijing Key Laboratory of Low Dimensional Semiconductor Materials and Devices, Beijing 100083, China (e-mail: myzhong@semi.ac.cn).

Huan Li, Daibing Zhou, Fei Guo, Dan Lu, Lingjuan Zhao, and Song Liang are with the Key Laboratory of Optoelectronic Materials and Devices, Institute of Semiconductors, Chinese Academy of Sciences, Beijing 100083, China, also with the Center of Materials Science and Optoelectronics Engineering, University of Chinese Academy of Sciences, Beijing 100049, China, and also with the Beijing Key Laboratory of Low Dimensional Semiconductor Materials and Devices, Beijing 100083, China (e-mail: huanli@semi.ac.cn; dbzhou@semi.ac.cn; guofei11@semi.ac.cn; ludan@semi.ac.cn; ljzhao@semi.ac.cn; liangsong@semi.ac.cn).

Kun Yang is with the College of Electronic Information, Zhengzhou University of Light Industry, Zhengzhou 450000, China (e-mail: yyyk2002@163.com).

Digital Object Identifier 10.1109/JPHOT.2024.3406064

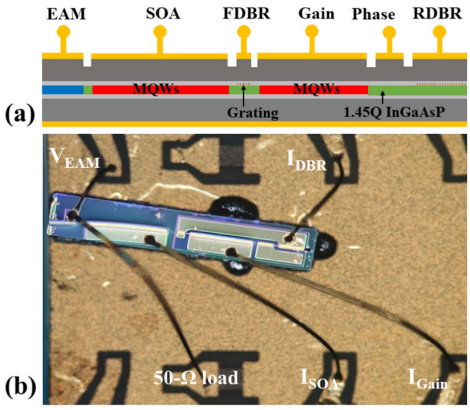

Fig. 2. Device schematic structure (a). Optical image of the TEML laser (b).

using butt-joint material growth technology and operates at a wavelength of 1.5 μm. The characteristic temperature of the device is 83 K, which is notably higher than that of a laser based on InGaAsP MQWs. At 25°, the electro-absorption modulator (EAM) of the laser has a small-signal modulation bandwidth exceeding 27 GHz, which is notably higher than that for a TEML device having the same structure but InGaAsP MQW active material. 25 Gb/s NRZ data modulations have been demonstrated at different wavelengths in the 12.56 nm tuning range of the device. To achieve 10E-10 bit error rate (BER), the power penalty after 5 and 10 km fiber transmission are 1 and 3 dB, respectively.

II. Device Fabrication

Fig. 2(a) shows a schematic cross-section structure of the TEML device, which consists of a 200 μm long rear DBR section, a 100 μm phase section, a 400 μm gain section, a 50 μm front DBR section, a 500 μm semiconductor optical amplifier (SOA) section, and a 150 μm EAM section. The SOA is used to compensate the optical loss in the DBR and EAM sections.

The device material is grown by a four-step metal organic chemical vapor deposition (MOCVD) process. During the first MOCVD step, MQWs for the gain and SOA sections are grown on an n-type InP substrate. The MQWs consist of six compressively strained InGaAlAs quantum wells and seven tensile-strained InGaAlAs barriers and are sandwiched between two 100 nm thick graded index separate confinement heterostructure (GRIN-SCH) InGaAlAs layers. The peak of the photoluminescence spectrum of the MQWs is at 1535 nm. After the gain and SOA sections are covered with a SiO_2 film, the MQWs in the rest area are removed selectively. In the second step MOCVD, EAM MQWs with a bandgap wavelength of 1490 nm is grown. The EAM MQWs consists of nine compressively strained InGaAlAs quantum wells and ten tensile strained InGaAlAs barriers. In the third step of MOCVD, a 450 nm thick InGaAsP bulk material having 1.45 μm bandgap wavelength is grown to be butt-jointed with the MQWs. As shown in Fig. 2(a), the InGaAsP material is used for the isolation region between the EAM and SOA, the phase and the DBR sections. Finally, p InP cladding layer and InGaAs contact layer are grown after gratings are formed by electron beam lithography and dry etching in the DBR sections.

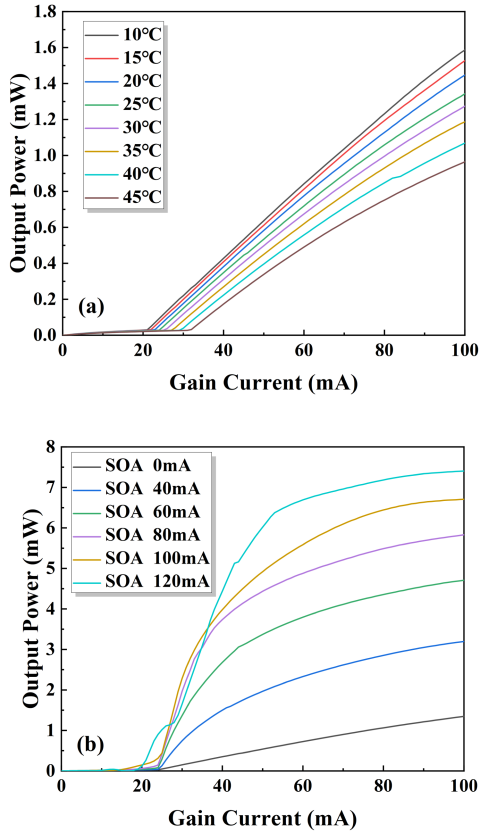

Fig. 3. Optical power as a function of gain current at different temperature when the SOA is set at 0 mA current (a) and at different SOA current at 25° (b). For all the measurements, the EAM is not biased.

A surface ridge waveguide is adopted for the device. The ridge waveguides are tilted at the SOA region for 7° to minimize the facet reflection. The isolation resistance between EAM and SOA is approximately 8400 Ω. A 2 μm thick SiO_2 layer is placed under the contact pad of the EAM to reduce the capacity thus enhancing the modulation bandwidth. Fig. 2(b) shows an optical graph of a fabricated device. For the device, the electrodes of the two DBR sections are connected. For testing, the laser is soldered onto an AlN heatsink and the device temperature is set at 25 °C by a thermo-electric cooler unless specified.

III. Result and Discussions

Fig. 3(a) shows the optical power as a function of the gain current measured from the unbiased EAM facet by an integrating sphere at temperature ranging from 10 °C to 45 °C when the SOA current is set to 0 mA. As can be seen, the threshold current of the laser increases from 21 mA to 32 mA in the temperature range. The corresponding characteristic temperature of the device is 83 K, which is notably larger than that for a laser having InGaAsP MQWs as active material [13], [14] because of the larger conduction band offset between well and barriers for the InGaAlAs MQWs. When the EAM is unbiased, the output power of the laser as a function of the gain current at different SOA current is shown in Fig. 3(b). By setting the gain and SOA currents to 100 mA and 120 mA, respectively, an over

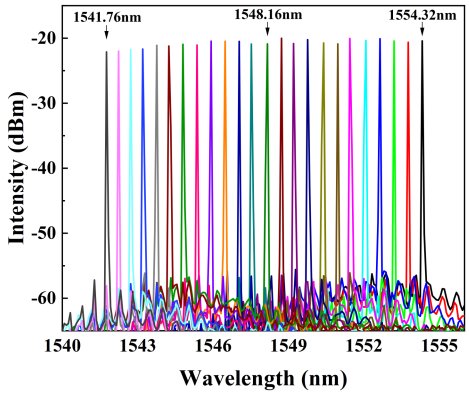

Fig. 4. Typical optical spectra obtained from the TEML laser at 25 °C.

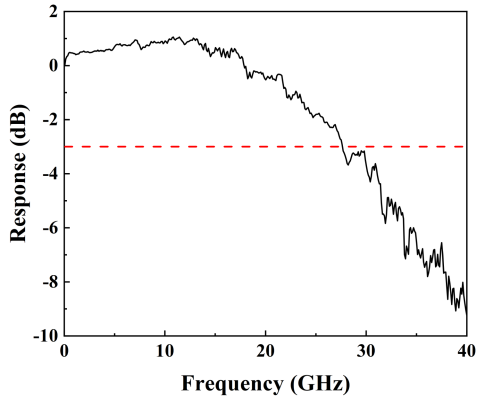

Fig. 5. Curve of the TEML laser at 25 °C when the SOA section, gain section, phase section, and DBR section were biased at 100, 120, 0, and 0 mA, respectively.

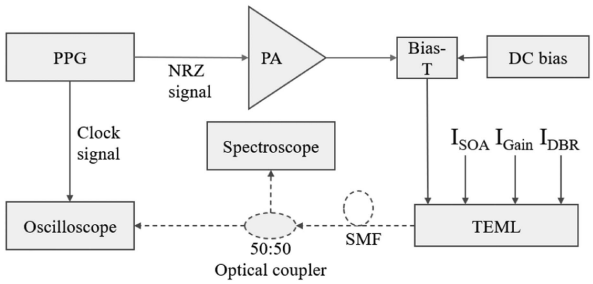

Fig. 6. Experimental setup used to the NRZ transmission characteristics of the TEML laser.

7 mW optical power can be collected. The relatively low output power can be attributed to the unoptimized butt joint interface between each adjacent two sections of the device. This induces a large optical loss in the device cavity. By further optimizing the butt joint growth process, including material selective etching, MOCVD growth parameters such as temperature, pressure and growth rate, a low loss interface between different materials can be obtained.

At the above bias condition, a wavelength tuning range of 12.56 nm which is from 1554.32 nm to 1541.76 nm can be achieved when the DBR current is increased from 0 to 60 mA. This tuning range is similar to the TEMLs having InGaAsP MQWs as active material [13], [14]. The large tuning range can be attributed to the InGaAsP DBR material having the long bandgap wavelength. For a DBR laser, the inject current induced wavelength change is proportional to the bandgap wavelength of the DBR material [20]. A thin film heater can be formed in the DBR section to enlarge the wavelength tuning range by thermal tuning. For DBR lasers, by adjusting the DBR current and the phase section current at the same time, any wavelength within the tuning range can be accessed. Fig. 4 shows the typical optical spectra obtained within the tuning range, all of which have over 35dB side mode suppression ratio (SMSR), indicating a good single mode emission performance. For the spectra measurements, the DBR section current is varied between 0 and 60 mA. The phase current is also adjusted between 0 and 30 mA to tune the wavelength finely.

At −5 V bias, the EAM has a larger than 14 dB static extinction ratio within the wavelength tuning range. A 50 GHz vector network analyzer is used to analyze the small signal modulation characteristics of the TEML device. The modulation signal is applied onto the device through a GSG probe. The modulated output optical signal of the laser is converted to electrical signal by a PIN PD (Finisar XPDV2120R) before being fed into the vector network analyzer. During the test process, the gain, SOA, DBR, and phase currents are 100, 120, 0, and 0 mA, respectively. The EAM bias voltage is −3 V. Figure 5 shows the electro-optic response curve of the EAM of the laser, which shows an over 27 GHz 3 dB modulation bandwidth. In contrast, for the InGaAsP MQW TEML device having the same EAM length and contact pad area [13], the modulation bandwidth is only 14 GHz though a 2 μm thick polymide is formed below the EAM pad. The bandwidth can be further enhanced by increasing the length of the wire between the EAM contact pad and the matching resistance [14] and by replacing SiO_2 under the contact pad with materials having lower dielectric constant. For different wavelengths, a similar bandwidth can be obtained for the device. Compared to the InGaAsP MQWs, the InGaAlAs MQWs have a larger conduction band offset and smaller valence band offset, which leads to stronger confinement for electrons and lower confinement for holes, favoring better high frequency characteristics for modulators [21].

Data modulation and transmission tests of the TEML device are then conducted. As shown in Fig. 6, non-return-to-zero (NRZ) pseudo-random bit sequence with a byte length of 2^7-1 is generated by a commercial pulse pattern generator (PPG, SHF-12125B). After being amplified by an RF power amplifier, the signal is combined with a DC bias voltage by a Bias-T before being fed to the EAM. The modulated optical signal, which is transmitted through an optical fiber, is split into two parts by an optical coupler. One part of the signal is fed into a sampling oscilloscope for eye diagram measurement. The other part is fed into a spectrometer for spectral monitoring. During the test process, the output wavelength of the laser is tuned by varying the DBR current.

Fig. 7 shows the 25 Gb/s eye diagrams obtained from the TEML device for back-to-back (BTB), and after 5 km and 10 km

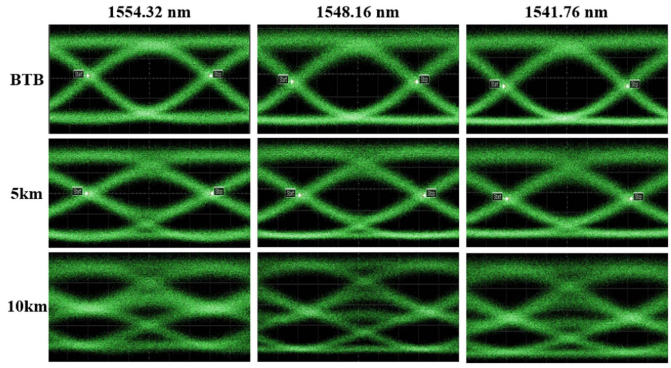

Fig. 7. 25 Gb/s eye diagrams of TEML laser for BTB, 5 and 10 km transmission when the tuned wavelength is 1554.32, 1548.16, and 1541.76 nm.

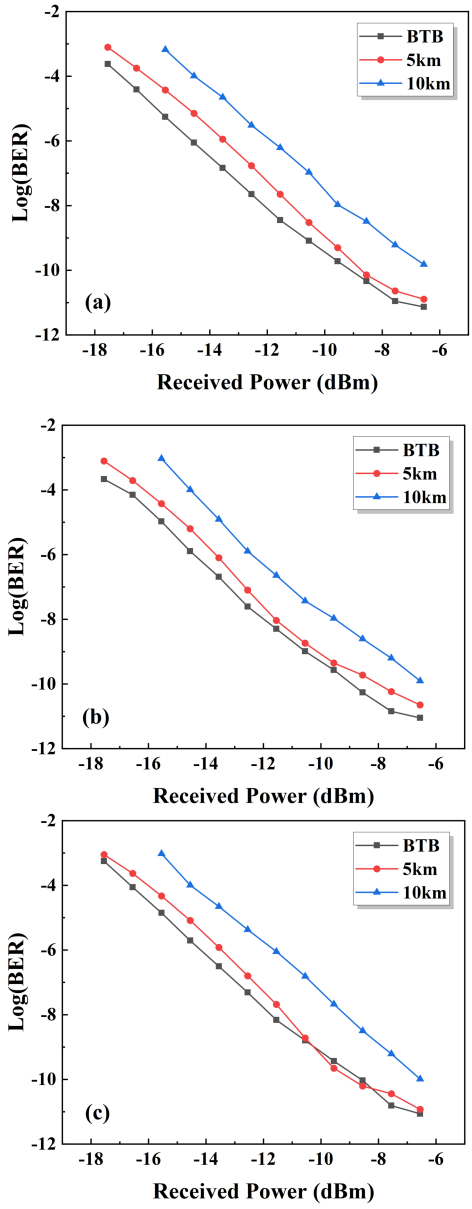

Fig. 8. BER performance at 25 Gb/s NRZ data modulation for wavelengths of 1554.32 nm (a), 1548.16 nm (b), and 1541.76 nm (c).

of standard single mode fiber transmissions when the wavelengths are tuned to 1554.32 nm, 1548.16 nm, and 1541.76 nm, respectively. As can be seen, clearly opened eye diagrams can be obtained at all the three typical wavelengths for the BTB and 5 km conditions. After 10 km of fiber transmission, the eyes start to be vague, but still distinguishable.

The BER performance of the device at 25 Gb/s NRZ data modulation is shown in Fig. 8. A Finisar XPDV2120R PD is used to convert the optical signals to electrical signals. As can be seen, error free (10E-10) transmission can be obtained for all the different conditions. The 5 km and 10 km transmission power penalty when compared with the BTB transmission is less than 1 dB and 3 dB, respectively, for all the three tested wavelengths. The data modulation performance is comparable to that for the InGaAsP device reported in reference [14], whose bandwidth, however, needs to be enlarged by a long bonding wire between the EAM and the matching resistance.

IV. Conclusion

In summary, we report the fabrication of a first TEML device based on InGaAlAs MQW material. The device operates at a wavelength of 1.5 μm and an over 12 nm wavelength tuning range can be obtained. The characteristic temperature of the device is over 83 K, which is notably higher than that of a laser based on InGaAsP MQWs. At 25 °C, the EAM of the device has a small-signal modulation bandwidth exceeding 27 GHz, which is higher than the bandwidth for a TEML device having the same structure but InGaAsP MQW active material. At 25 Gb/s NRZ data modulation, lower than 10E-10 bit BER can be obtained for up to 10 km fiber transmission. The device is a promising low-cost light source for future high capacity WDM optical communication systems.

References

[1] R. Bonk et al., "50G-PON: The first ITU-T higher-speed PON system," *IEEE Commun. Mag.*, vol. 60, no. 3, pp. 48–54, Mar. 2022.
[2] D. Zhang, D. Liu, X. Wu, and D. Nesset, "Progress of ITU-T higher speed passive optical network (50G-PON) standardization," *J. Opt. Commun. Netw.*, vol. 12, no. 10, pp. D99–D108, 2020.
[3] D. Nesset, "Next generation PON technologies: 50G PON and beyond (Invited)," in *Proc. IEEE Int. Conf. Opt. Netw. Des. Model.*, 2023, pp. 1–6.
[4] R. Rosales et al., "Achieving high budget classes in the downstream link of 50G-PON," *J. Opt. Commun. Netw.*, vol. 13, no. 8, pp. D13–D21, 2021.
[5] R. Rosales, I. N. Cano, D. Nesset, R. Brenot, and G. Talli, "50G-PON downstream link up to 40 km with a 1342 nm integrated EML+SOA," *IEEE Photon. Technol. Lett.*, vol. 34, no. 6, pp. 306–308, Mar. 2022.
[6] X. Chen et al., "A high power electro-absorption modulated laser integrated with SOA suitable for 50G PON application," *IEEE Photon. Technol. Lett.*, vol. 36, no. 1, pp. 5–7, Jan. 2024.
[7] W. Kobayashi et al., "50-Gb/s direct modulation of a 1.3-μm InGaAlAs-based DFB laser with a ridge waveguide structure," *IEEE J. Sel. Topics Quantum Electron.*, vol. 19, no. 4, Jul./Aug. 2013, Art. no. 1500908.
[8] D. Anthon, J. D. Berger, and A. Tselikov, "C+L band MEMS tunable external cavity semiconductor laser," in *Proc. Opt. Fiber Commun. Conf.*, 2004, pp. 761–.
[9] X. Han, Q. Cheng, F. Liu, and Y. Yu, "Numerical analysis on thermal tuning efficiency and thermal stress of a thermally tunable SG-DBR laser," *IEEE Photon. J.*, vol. 8, no. 3, Jun. 2016, Art. no. 1501512.
[10] D.-B. Zhou, S. Liang, L.-S. Han, L.-J. Zhao, and W. Wang, "Widely tunable two-section directly modulated DBR lasers for TWDM-PON system," *Chin. Phys. Lett.*, vol. 34, no. 3, 2017, Art. no. 034204.

[11] O. K. Kwon, C. W. Lee, S. I. Park, K. S. Park, and K. S. Kim, "100-Gb/s/λ PAM-4 EAM-integrated DBR-LD supporting multiple sub-channels within 1.29 μm window," *J. Lightw. Technol.*, vol. 41, no. 18, pp. 6015–6020, Sep. 2023.

[12] T. Yamamoto, "High-speed directly modulated lasers," in *Proc. Opt. Fiber Commun. Conf.*, 2012, Paper OTh3F.5.

[13] L. Han et al., "Electroabsorption-modulated widely tunable DBR laser transmitter for WDM-PONs," *Opt. Exp.*, vol. 22, no. 24, pp. 30368–30376, 2014.

[14] Y. Liu et al., "Up to 50 Gb/s modulation of an EAM integrated widely tunable DBR laser," *Opt. Exp.*, vol. 29, no. 3, pp. 4523–4529, 2021.

[15] D. Zhou, S. Liang, L. Zhao, H. Zhu, and W. Wang, "High-speed directly modulated widely tunable two-section InGaAlAs DBR lasers," *Opt. Exp.*, vol. 25, no. 3, pp. 2341–2346, 2017.

[16] N. Sasada et al., "Wide-temperature-range (25–80 °C) 53-gbaud PAM4 (106-Gb/s) operation of 1.3-μm directly modulated DFB lasers for 10-km transmission," *J. Lightw. Technol.*, vol. 37, no. 7, pp. 1686–1689, Apr. 2019.

[17] D. Zhou et al., "50 Gb/s electro-absorption modulator integrated with a distributed feedback laser for passive optical network systems," *Photonics*, vol. 9, no. 10, 2022, Art. no. 780.

[18] C. E. Zah, "A recap of high performance AlGaInAs/InP laser development history," in *Proc. IEEE 28th Int. Semicond. Laser Conf.*, 2022, pp. 1–2.

[19] N. C. Frateschi, J. Zhang, R. Jambunathan, W. J. Choi, C. Ebert, and A. E. Bond, "Uncooled performance of 10-Gb/s laser modules with InGaAlAs-InP and InGaAsP-InP MQW electroabsorption modulators integrated with semiconductor amplifiers," *IEEE Photon. Technol. Lett.*, vol. 17, no. 7, pp. 1378–1380, Jul. 2005.

[20] L. Yu et al., "A widely tunable directly modulated DBR laser with high linearity," *IEEE Photon. J.*, vol. 6, no. 4, Aug. 2014, Art. no. 1501308.

[21] D. Zhou, Y. He, D. Lu, S. Liang, L. Zhao, and W. Wang, "25 Gb/s data transmission using a directly modulated InGaAlAs DBR laser over 14 nm wavelength tuning range," *Photonics*, vol. 8, no. 3, 2021, Art. no. 84.